

Araştırma Makalesi / Research Article

## Evaluation of the Safe Mud Weight Window: Wellbore Stability Analysis, Rumaila Oilfield, Southern Iraq

*Güvenli Çamur Ağırlık Penceresinin Değerlendirilmesi: Bir Kuyu Stabilite Analizi, Rumaila Petrol Sahası, Güney Irak*

Saad W. SAADI<sup>1\*</sup> , Nihad Saoud ALJUBOORI<sup>2</sup> , Mohammed Zainel QADER<sup>3</sup>

Elaf Mohammed SHAKIR<sup>3</sup> , Ahmed Ibrahim AL-NAEMI<sup>3</sup> , Lizan Ahmed SALEH<sup>3</sup>

<sup>1</sup>University of Mosul, College of Petroleum and Mining Engineering, Department of Petroleum Reservoir Engineering, Mosul/ Iraq

<sup>2</sup>University of Mosul, College of Petroleum and Mining Engineering, Department of Mining Engineering, Mosul/ Iraq

<sup>3</sup>North Oil Company, Kirkuk/ Iraq

Geliş (Received): 11/05/2025 / Düzeltme (Revised): 04/07/2025 / Kabul (Accepted): 06/09/2025

### ABSTRACT

Wellbore instability leads to severe operational interruption and financial losses during the drilling process, resulting in additional non-productive periods in the petroleum and natural gas sector. This study was undertaken to comprehend the nature of wellbore stability challenges at the Rumaila oilfield, southern Iraq for the purpose of enhancing well design. The aim of this study was to create a one-dimensional geomechanical model. Measurements from open hole well logs were required to create the model. Three failure criteria including Mohr-Coulomb, Mogi-Coulomb, and Modified Lade were utilized to figure out the minimum mud weight required for a solid (stable) wellbore wall and also to analyze borehole breakouts. To improve the precision of the geomechanical model, a comparison was made between the projected instability profile of the borehole with the observed failure of the borehole, as reported by the caliper log. The findings indicate that the Mogi-Coulomb criterion more accurately predicts well failure than the other two criteria, establishing it as the superior method for forecasting the rock lowest boundary of mud weight window in the study area. The study of wellbore instability indicated that low and vertical wells with a deviation of less than 40° are safer and more stable. The suggested mud weight was increased to 10.5 ppg to mitigate the majority of instability issues. The findings will aid in planning development for wells adjacent to the examined region, and hence reduce non-productive time and costs.

**Keywords:** Geomechanical model, wellbore instability, one-dimensional geomechanical model, safe mud weight window, Mogi-Coulomb criterion

### ÖZ

*Kuyu kararsızlığı, sondaj sürecinde ciddi operasyonel kesintilere ve mali kayıplara yol açarak petrol ve doğal gaz sektöründe ek üretimsiz zamanlara neden olur. Bu çalışma, kuyu tasarımı iyileştirmek amacıyla Irak'ın güneyindeki Rumaila petrol sahasında kuyu stabilitesi sorunlarının doğasını anlamak için yürütülmüştür. Çalışmanın*

amacı, bir boyutlu jeomekanik model oluşturmaktır. Modeli geliştirmek için açık kuyu loglarından elde edilen ölçümlere ihtiyaç duyulmuştur. Kuyu duvarının sağlam kalması için gerekli minimum çamur ağırlığını belirlemek ve kuyu genişlemelerini analiz etmek amacıyla Mohr–Coulomb, Mogi–Coulomb ve Modifiye Lade olmak üzere üç farklı yenilme kriteri kullanılmıştır. Jeomekanik modelin doğruluğunu artırmak için, kuyu için öngörülen duraysızlık profili, kaliper logu ile raporlanan gözlenen kuyu başarısızlığı ile karşılaştırılmıştır. Bulgular, çalışma alanında çamur ağırlığı aralığının alt sınırını tahmin etmede Mogi–Coulomb kriterinin diğer iki kriterden daha doğru sonuç verdiğini, dolayısıyla en uygun yöntem olduğunu göstermektedir. Kuyu duraysızlığı analizi, düşük eğimli ve 40°'den az sapmaya sahip dik kuyuların daha güvenli ve daha sağlam olduğunu ortaya koymuştur. Duraysızlıkların büyük bölümünü azaltmak için önerilen çamur ağırlığı 10,5 ppg'ye yükseltilmiştir. Elde edilen sonuçlar, incelenen bölgeye yakın kuyuların planlanmasına yardımcı olacak, böylece üretimsiz zamanların ve maliyetlerin azaltılmasına katkı sağlayacaktır.

**Anahtar Kelimeler:** Jeomekanik model, kuyu duysarsızlığı, tek boyutlu jeomekanik model, güvenli çamur ağırlık penceresi, Mogi-Coulomb kriteri

## INTRODUCTION

Geomechanics is an essential field in engineering that focuses on analyzing the connection between rocks and stress distribution. In addition, geomechanics investigates the impact of a number of elements on rock, such as changes in pressure, temperature, and related environmental conditions (AlShibli and Alrazzaq, 2022; Balaky et al. 2023).

In the last few decades, developments in the oil and gas industry drove geomechanics specialists and researchers to increase the drilling penetration rate and implement deviated and horizontal drilling technology (Ma et al., 2015; Rafieepour et al., 2020; Yan et al., 2022; Ding et al., 2023; Liu, et al., 2024; Wei et al., 2024). However, wellbore instability problems were exacerbated (Hosseini et al., 2023; Kianoush et al., 2023; Pirhadi, et al., 2023; Wang et al., 2023). To address this, scientists developed theories, constitutive models, correlations, failure criteria, and digital applications. These tools were used to determine pore pressure, in-situ stresses, and rock mechanical properties to analyze wellbore stability (Al-Juraisy and Al-Majid, 2021; Wang et al., 2023). This analysis contributed to mitigating the challenges associated with wellbore instability.

In spite the fact that there is a noticeable advances and newly developed technologies in the petroleum and natural gas sectors, the issue of wellbore instability remains one of the most formidable challenges faced throughout the drilling and completion processes (Al-Qahtani, and Zillur; 2001, Mohiuddin, et al., 2001; Abalioglu, et al., 2011; Bagheri, et al., 2021; Almasi, and Mohsenipour, 2022). This leads to increases in operational expenses and non-productive time (NPT) (Zeynali, 2012; Manshad et al., 2022; Ounegh, et al., 2024). Therefore, wellbore stability has become a crucial part of planning wells (Boutt, et al. 2011). Wellbore instability occurs when the applied mud weight is insufficient to counteract the compressive strength of the surrounding formations, leading to phenomena such as wellbore expansion and collapse. Also, if the weight of the mud exceeds the pressure at which the formation fractures, it will induce fracturing, resulting in lost circulation. Moreover, natural fractures of any size could have a substantial impact on the condition of in-situ stresses and other stresses that are caused by the borehole annulus (Ewy, 1999). Consequently, there are increases in the costs of drilling operations and NPT. However, these problems can be avoided by adequate internal wellbore pressure (mud weight). Other parameters must

be considered such as borehole inclination and direction, concerning in-situ stresses to avoid the effect of the wellbore angle on wellbore failure and the correct selection of mud weight windows (Al-Ajmi and Zimmerman, 2006; Chandong, et al., 2006; Algburi, et al., 2023). An overall rise in wellbore slope results in an elevation of breakout pressure due to the angle of inclination and azimuth (Plumb and Richard, 1985).

Accurately determining both regional and local in-situ stresses is crucial for effective well design to mitigate wellbore instability challenges such pipe blockage, fluid loss, and inadequate hole cleaning (Al-Rubaye and Hamd-Allah, 2019). Recently, considerable attention has been given to geomechanics for the sake of solving wellbore instability problems by utilizing a numerical method that can greatly reduce the wellbore instability through building mechanical earth models (MEM) (Gstalder and Raynal, 1966). The model can predict the state of stress and mechanical rock properties (strength and elastic) around the wellbore. MEM utilize data from core laboratory tests, drilling mud reports, and geological studies, as well as daily and final well drilling reports for the investigated area. Stress and rock properties are used to select safe mud weight and orientation of wellbore to design a stable trajectory by using an appropriate failure criterion. The parameters presented in this study are derived from the analysis of outputs obtained from a one-dimensional mechanical earth model (1DMEM) (Ounegh, et al., 2024).

The safe mud weight window is an important component in preventing different drilling issues, including wellbore instability, collapse, wash-out, tightening, kicks, increased drilling costs, production stops, and even well loss. The safe mud weight window ensures the stability of the wellbore and avoids the occurrence of lost

circulation. To ensure wellbore stability and control these stresses, it is necessary to drill the well using a mud weight that is safe (Boutt et al. 2011).

The aim of this research is to study the pore pressure prediction and identify the size and direction of in-situ primary stresses (vertical stress, horizontal stresses). A one-dimensional geomechanical earth model (1D MEM) was built using Techlog well-log interpretation software. In addition, appropriate failure criteria were selected to analyze wellbore stability based on the outcomes of 1D-MEM. Finally, the safe mud weight window (SMWW) was designed for different formations based on the reservoir and geomechanical considerations.

## STUDY AREA AND STRATIGRAPHIC SETTING

The Rumaila oilfield was discovered in 1953 and is regarded as one of the largest oilfields globally; thereby, earning the designation of a supergiant field. It is situated around 50 kilometers west of Basra, south of Iraq. Rumaila oilfield has an area of 1,600 km<sup>2</sup>, extending about 80 km in the north-south direction towards the Iraq-Kuwait border and 20 km in the east-west direction towards the West Qurna oilfield, as seen in Figure 1. It comprises two anticlines: the North Dome and the South Dome. Rumaila reservoir includes stacked sandstone and carbonate up to 4 km thick dated to the Cretaceous (ROO, 2016).

The lithologic column for the Rumaila oilfield extends from the Dibdiba Formation to the Zubair Formation, as shown in Figure 2 (Bradley, 1979; Al-Agaili, 2012). The lithologic column for the model begins at a depth of 1834 m with the Sadi Formation and extends to a depth of 3340 m with the lower Zubair Formation,

which is the interval of interest. This sector has two primary pay zones, namely the Mishrif and Zubair Formations (Al-Agaili, 2012).

## PROBLEM STATEMENT

The problems arise at an 8 ½ inch portion, which corresponds to the production section per the well design for Rumaila oilfield. Four unstable shale horizons are present, namely Tanuma, Ahmadi, Nahr-Umr, and Zubair/Upper Shale Formations. Tanuma and Upper Shale of Zubair are the formations that cause the most significant problems. Wellbore instability has

different forms in the problematic formations, as listed below (ROO, 2016):

1. Tanuma: mainly chemical, instability develops over time and creating splintery cavings.
2. Zubair /Upper Shale: stress-related, instantaneous with angular to blocky cavings.

Zubair Formation is the interval of interest and these problems lead to high NPT compared with other drilling operations in the same section, as shown in Figure 3.

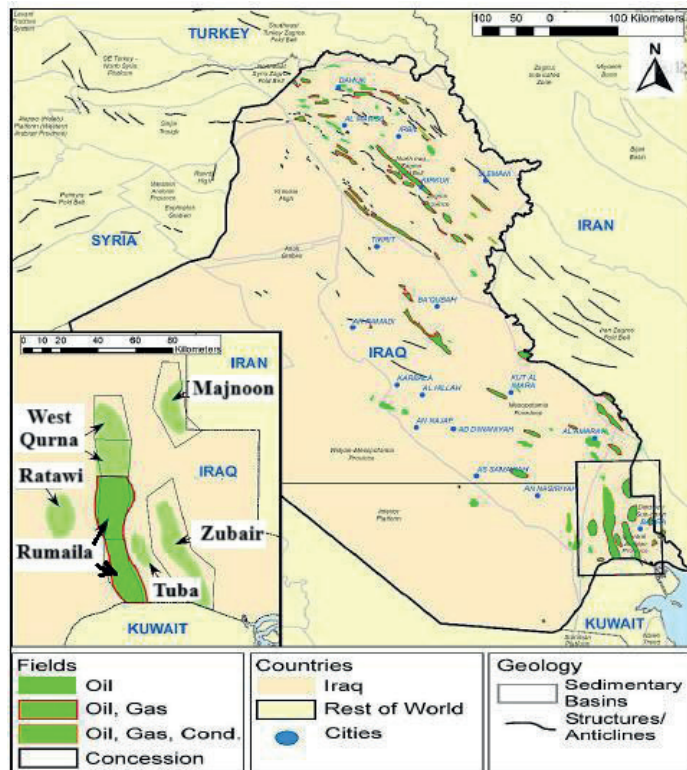


Figure 1. The distribution of oil and gas fields across Iraq, with an emphasis on major production regions, particularly focusing on the study area—Rumaila Oilfield in southern Iraq (ROO, 2016).

Şekil 1. Harita, Irak genelindeki petrol ve doğalgaz sahalarının dağılımını göstermekte olup, başlıca üretim bölgelerine vurgu yapılmaktadır. Özellikle çalışma alanı olan güney Irak'taki Rumaila Petrol Sahası'na odaklanılmaktadır (ROO, 2016).



Age		Group	Formation	Lithology	Description	Average thickness (m)		
Period	Epoch							
Tertiary	L. Miocene-Recent	Kuwait	Dibdibba		Sand & pebble	200		
	Early-M Miocene		Lower Fars		Clay St, Lst arg	170		
			Ghar		Sand & subround pebble occ Clay	110		
	M-L Eocene	Hasa	Dammam		Dolomite, porous vuggy	210		
	Paleocene-Early Eocene		Rus		Anhydrite, white, massive Interbedded w\ Dolomite	165		
Umm-Er-Radhuma				Dolomite grey saccharoidol, inpart anhydritic	450			
Cretaceous	Late Cretaceous	Aruma	Tayarat		Bituminous Shale at top, Dolomite grey	220		
			Shiranish		Limestone marly	120		
			Hartha		Lst, gloc, Dol, porous, locally vuggy, Lst, grey, arg.	180		
			Sadi		Limestone white, chalcky, fine compact	260		
			Tanuma		Shale: black-brown fissile	50		
			Khasib		Limestone: grey shaly	45		
			Middle Cretaceous	Wasia	Mishrif		Limestone: white detrital, porous, rudist	150
					Rumaila		Limestone: grey, marly	100
					Ahmadi		Shale: Dark grey, fissile w/ Limestone: grey	140
	Mauddud				Limestone grey	110		
	Nahr Umr				Shale black inter. w/ Sst	270		
	Early Cretaceous	Thamama			Shuaiba		Lst, Dolomaite Fracture	85
			Zubair		Shale, fissile, w/ sandstone fine-m. grained, Silt st, Clay st.	400		
			Ratawi		Limestone with streaks of Shale	200		
			Yamama		Limestone, light grey	120		
Jurassic	Upper Jurassic		Sulaiy		Limestone, argillaceous and marly	300		

Figure 2. Stratigraphic column for Rumaila oilfield (Bradley, 1979; Al-Agaili, 2012).

Şekil 2. Rumaila petrol sahasına ait stratigrafik kesit (Bradley, 1979; Al-Agaili, 2012).

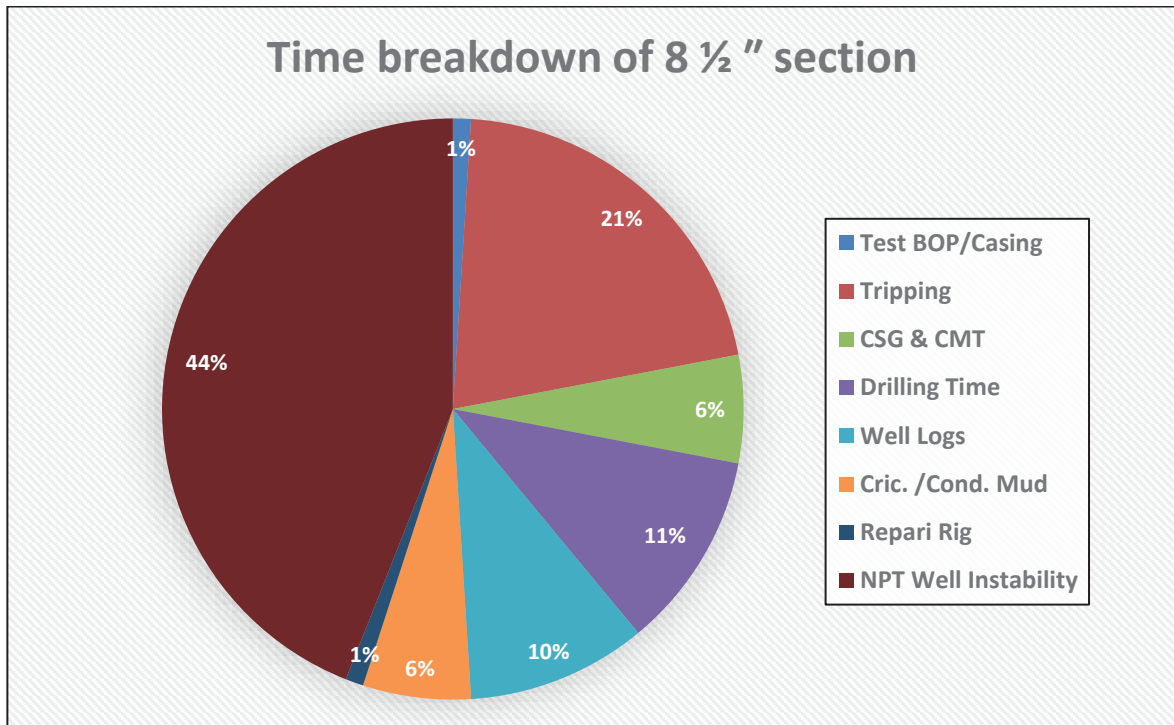


Figure 3. Time breakdown of 8½ " section (ROO, 2016).

Şekil 3. 8 ½ " kesitinin zaman dağılımı (ROO, 2016).

## METHODOLOGY

This study utilized samples obtained from Rumaila oilfield, operated by the South Oil Company in Iraq (Nader et al., 2022; Ali, 2023). The geomechanical model study for Rumaila oilfield was accomplished by using an integrated method comprising four primary phases, as seen in Figure 4. The first phase included gathering the necessary data for model creation, including logs measuring density, gamma ray, shear wave velocities, compression wave velocities, caliper, and bit size. Additionally, data measured with laboratory core testing was collected and its

validity was verified. The next phase included the building of 1D mechanical earth model (1D-MEM). The third phase consisted of calculations from 1D-MEM profiles, such as mechanical properties of rock, pore pressure and magnitudes, and also the direction of far-field stress. Finally, wellbore stability was analyzed by comparing the failure prediction of the wellbore employing multiple failure criteria, with the actual wellbore profile, obtained from the caliper log. This analysis will help to determine suitable orientation (inclination and azimuth) and safe mud weight range for drilling new wells in nearby locations.

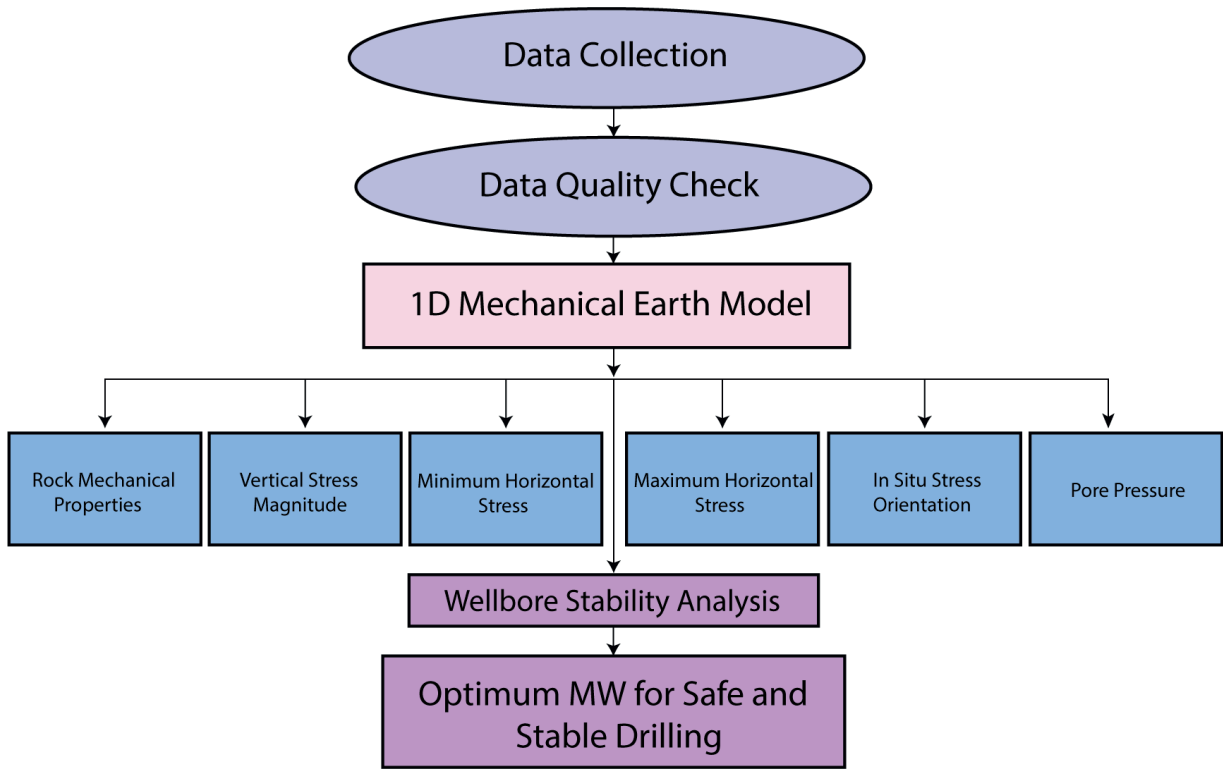


Figure 4. Methodological workflow for the study.

Şekil 4. Çalışman metodolojisinin iş akışı.

### Geomechanical Model (Mathematical Approach)

Failure criteria formulations for wellbore stability are given below.

#### 1. Mohr-Coulomb Failure Criterion (2D)

This criterion is commonly employed and postulates that failure occurs when the shear stress acting on a plane exceeds a critical threshold, which is determined by the material's cohesion and internal angle of friction (Aadnoy and Looyeh, 2019).

$$\tau = c + \sigma_n \cdot \tan(\varphi) \quad (1)$$

In terms of principal stresses:

$$\frac{(1 + \sin(\varphi))}{(1 - \sin(\varphi))} + \frac{(2c \cdot \cos(\varphi))}{(1 - \sin(\varphi))} \quad (2)$$

#### 2. Mogi-Coulomb Failure Criterion (3D)

This model represents an extension of the Mohr-Coulomb criterion by incorporating the influence of the intermediate principal stress ( $\sigma_2$ ); thereby, enhancing the accuracy of failure predictions under true triaxial stress conditions (Aadnoy and Looyeh, 2019).

$$\tau_{\text{oct}} = a + b \cdot \sigma_{m,2} \quad (3)$$

where:

$$\tau_{oct} = \sqrt{\frac{1}{3} \cdot ((\sigma_1 - \sigma_2)^2 + (\sigma_2 - \sigma_3)^2 + (\sigma_3 - \sigma_1)^2)}$$

$$\sigma_{m,2} = (\sigma_1 + \sigma_3) / 2$$

### 3. Modified Lade Failure Criterion

This criterion accounts for all three principal stresses and is considered more suitable for wellbore stability in brittle formations (Ewy, 1999).

$$(I_1 / \sqrt{I_3})^2 = k \quad (4)$$

where:

$$I_1 = \sigma_1 + \sigma_2 + \sigma_3$$

$$I_3 = \sigma_1 \cdot \sigma_2 \cdot \sigma_3$$

$k$  = material constant determined from lab tests

The current study employs a geomechanical model for reliability and validity in the determination of wellbore stability (Figure 5). Mechanical characteristics of rock, pore pressure, and in-situ stress are the primary geomechanical model components (AlShibli and Alrazzaq, 2022). The mud weight window and wellbore trajectory are two main output parameters of the geomechanical model that can be improved to limit the incidence of tensile failure in the wellbore and lower the high cost of NPT (Hoseinpour and Riahi, 2022).

Geomechanical problems can be addressed via the construction of 1D-MEM and 3D-MEM, which ascertain the size and direction of far-field stresses, estimate pore pressure, and evaluate the mechanical characteristics of rocks.

Several prevalent failure criteria, including Mohr-Coulomb, Mogi-Coulomb, and modified Lade, were used to anticipate the possible

lowest boundary of mud weight window for the wellbore in this rock formation. The Mohr-Coulomb failure criterion is categorized as a two-dimensional criterion, recognized for assessing wellbore breakout. Its fundamental assumption is a linear relationship between maximum and minimum stresses, disregarding intermediate stresses that could enhance the rock's strength. Consequently, experts determined that the Mohr-Coulomb criteria is an inadequate and overly cautious evaluation of suitable mud pressure. In true triaxial testing, the modified Lade and Mogi-Coulomb classifications are used to consider the effects of intermediate stress.

The primary components of the geomechanical model including vertical stress, mechanical stratigraphy (shale flag), pore pressure, rock properties (strength and elastic), and horizontal stresses (orientations and magnitudes) were used and developed by exploiting the relevant geomechanical data.

### Vertical Stress (overburden stress)

The vertical stress was computed by incorporating the derived densities from the bulk density log that covered the rocks, and using the following equation (Al-Ameri, 2015; Al-Ameri et al., 2020b; Al-Ameri et al., 2020c).

$$SV = g \int_0^Z \rho b(z) dz \quad (5)$$

Where is the bulk density of overlaying rocks integrated with respect to depth ( $Z$ ) and  $g$  denotes gravitational acceleration ( $m/s^2$ ). The missing density at the surface interval is extrapolated by using the equation below (2) (Gstalder and Raynal, 1966; Bell, 2003).



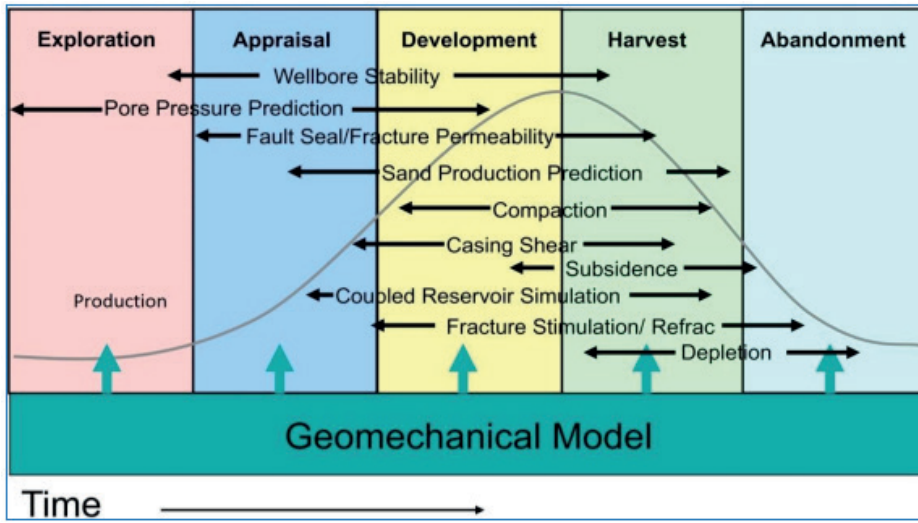


Figure 5. Geomechanics throughout the life of the field (Hoseinpour and Riahi, 2022).

Şekil 5. Saha ömrü boyunca jeomekanik (Hoseinpour ve Riahi, 2022).

Where is the bulk density of overlaying rocks integrated with respect to depth ( $Z$ ) and  $g$  denotes gravitational acceleration ( $m/s^2$ ). The missing density at the surface interval is extrapolated by using the equation below (2) (Gstalter and Raynal, 1966; Bell, 2003).

$$\rho_M = \rho_{mudline} + A_o \times (TVD - Air\ gap - Water\ depth)^\alpha \quad (6)$$

Where is the density at ground level in  $gm/cm^3$ ,  $\rho_{mudline}$  is the substance density at ground level (soil density  $1.65\ gm/cm^3$ ), air gap is the height of the rotary table from the ground (m), TVD is the true vertical depth (m), and  $A_o$  and  $\alpha$  are equation constants. The vertical stress profile is shown in the third track of Figure (6) for the studied formations.

### Shale Flag (Mechanical Stratigraphy)

A key outcome of MEM is the temporal characterization of rock mechanics, as well as the

optimal estimation of geomechanical parameters through the classification of rocks based on their mechanical stratigraphy. This allows differentiation between shale and non-shale formations, as illustrated in the second track of Figure 6 under the designation shale flag.

### Pore Pressure

In this study, pore pressure is utilized as it constitutes a fundamental component of the 1D-MEM, and plays a crucial role in estimating the size (magnitude) of in-situ horizontal stresses and predicting safe mud weight window to achieve wellbore stability particularly in the drilling phase. Pore pressure is estimated by direct and indirect methods. The direct method measures with the RFT and DST techniques. In the indirect method, the profile pore pressure is computed through merging the normal pressure and geo-pressure profiles. The profile of the hydrostatic pressure ( $P_h$ ) was computed through using equation number 7 and the profile of geo-

pressure in this study was calculated according to equation number 8, using the Eaton method (AlHusseini and Hamed-Allah, 2023). This equation was used to estimate the pore pressure in the shale formations (non-producing zone). The resultant profile was calibrated against actual pressure point measurements from indirect methods to minimize the uncertainty of the estimated pore pressure. This is demonstrated in the third track of Figure 6 under the name formation pressure for the studied formations.

$$P_{hydrostatic} = \int_0^z \rho_w g dz \quad (7)$$

$$P_p = \sigma_v - (\sigma_v - P_{pnorm}) * \quad (8)$$

### Rock Mechanical Properties

In this phase, both elastic and strength qualities were used for optimal assessment of the rock mechanical characteristics. The elastic properties encompass Young's modulus ( $E$ ), which quantifies the resistance of a rock sample to uniaxial stress; Poisson's ratio ( $\nu$ ), which assesses the rock's expansion relative to axial shortening; the shear modulus ( $G$ ), indicating the degree of rock deformation under shear stress; and the bulk modulus ( $K$ ), reflecting the material's hardness under volumetric compression. Strength attributes include the internal friction angle ( $\varphi$ ) which estimates rock failure; cohesive strength ( $S_o$ ) that specifies the degree of adhesion between interconnected molecules; tensile strength ( $T_s$ ) which indicates the rock's resistance; and unconfined compressive strength (UCS), which is the highest axial compressive stress in a triaxial test that a rock withstands before failing (Aadnoy and Looyeh, 2011; AlShibli and Alrazzaq, 2022). These properties are considered essential components in the determination of the magnitude of horizontal stresses, analysis of the

stability of the wellbore, and prediction of mud windows to achieve stable drilling.

The properties are assessed using direct laboratory procedures and indirect petrophysical methods, with direct methods often used to calibrate the estimated profiles derived from indirect methods.

In this study, the mechanical properties of rock were evaluated using indirect petrophysical methods based on three types of well logs: shear and compressional wave velocities, and bulk density, as expressed in equations 9 and 10. These were utilized to compute bulk and shear moduli ( $G$  and  $K$ ). Shear module ( $G$ ) is the measurement of the stiffness of material resistance against the applied shear stress. Bulk module ( $K$ ) measures the capability of the material to resist the change in volume when all sides of the material are under compression (AlHusseini and Hamed-Allah, 2023). Hence, the dynamic profiles of Young's modulus ( $E$ ) in Mpsi and Poisson ratio ( $\nu$ ) can be estimated from the two modules (shear and bulk), by using equations 11 and 12 sequentially (Schlumberger, 2018).

$$G_{dyn} = 13474.45 * \frac{\rho_b}{(\Delta t_{shear})^2} \quad (9)$$

$$K_{dyn} = 13474.45 * \left[ \frac{\rho_b}{(\Delta t_{comp})^2} \right] - \frac{3}{4} * G_{dyn} \quad (10)$$

where is  $\rho_b$  bulk density of the formation (g/cm<sup>3</sup>), ( $\Delta t_{shear}$ ) and ( $\Delta t_{comp}$ ) are acoustic travel time of shear and compressional in  $\mu\text{sec/ft}$ .

$$E_{dyn} = \frac{9 * G_{dyn} * K_{dyn}}{G_{dyn} + 3 * K_{dyn}} \quad (11)$$

$$\nu_{dyn} = \frac{3K_{dyn} - 2G_{dyn}}{6K_{dyn} + 2G_{dyn}} \quad (12)$$

These dynamic properties were used to estimate static elastic properties by applying

an appropriate correlation. In this study, John Fuller's correlation is employed to estimate the static Young's modulus profile. This describes a more realistic profile and is usually lower than the dynamic profile because of the influence of pore pressure, cementation, amplitude and also rate of stress-strain. The static Poisson's ratio was considered analogous to the dynamic form, as usually used in rock mechanics.

The estimated static profiles exhibit strong agreement with direct measurements obtained from laboratory tests of the investigated formations, as illustrated in the fourth track of Figure 6. Also, the profile of rock mechanical strength parameters has a good match with the direct measurements from core laboratory testing, as demonstrated in the fifth track of Figure 6 for the studied formations (Bell, 2003).

### Horizontal Principal Orientations and Stress Magnitudes

There are different indirect methods to determine the size of both maximum ( $\sigma_H$ ) and minimum ( $\sigma_h$ ) horizontal stress. In this study the pore elastic constitutive model is employed, which is considered the most successful method in determining magnitude of horizontal stresses (Moos et al., 2003), as demonstrated in the third track of Figure 6. The model equations are mainly based on the Young modulus, pore pressure, density, and rock deformation as expressed in equations 13 and 14 (Schlumberger, 2018).

$$\sigma_h = \frac{v}{1-v} * \sigma_v - \frac{v}{1-v} * \alpha P_o + \alpha P_o \frac{s*v}{1-v} * \varepsilon_h + \frac{v*E}{1-(v)^2} * \varepsilon_H \quad (13)$$

$$\sigma_H = \frac{v}{1-v} * \sigma_v - \frac{v}{1-v} * \alpha P_o + \alpha P_o \frac{s*v}{1-v} * \varepsilon_H + \frac{v*E}{1-(v)^2} * \varepsilon_h \quad (14)$$

$\sigma_h$  and  $\sigma_H$  are the minimum and maximum horizontal stresses, respectively,  $V$  refers to Poisson's ratio,  $\sigma_v$  represents the vertical stress,  $\alpha$  indicates Biot's coefficient (conventionally  $\alpha=1$ ), and  $E$  represents the static Young's modulus.  $P_p$  represents the pore pressure.  $\varepsilon_h$  and  $\varepsilon_H$  are the strain in the direction of  $\sigma_h$  and  $\sigma_H$ , respectively, as expressed in equations 15 and 16.

$$\varepsilon_h = \frac{\sigma_v * v}{E} * \left(1 - \frac{v^2}{1-v}\right) \quad (15)$$

$$\varepsilon_H = \frac{\sigma_v * v}{E} * \left(\frac{v^2}{1-v} - 1\right) \quad (16)$$

### Mud weight window

The mud weight window is a crucial outcome of wellbore stability analysis, including four essential parameters. These important parameters are delineated in relation to the mud pressure (Zhang, 2013; Bandara and Al-Ameri, 2024), as elucidated in Figure 7, which corresponds to the pressure equivalent of drilling mud weight:

1. Pore pressure: This refers to the formation pressure that must not surpass the drilling mud pressure to avert washout expansion, blowouts, or well kicks.
2. Shear failure pressure (Breakout pressure): minimum mud weight imposed must support the borehole wall to prevent breakout occurrence.
3. Formation breakdown pressure: The maximum pressure that the wellbore drilling mud pressure must not surpass to avert mud loss (formation ballooning) resulting from the initiation of an induced hydraulic crack on the wellbore wall.
4. The mud weight must not exceed the minimal horizontal stress to avert lost circulation resulting from the infiltration of wellbore fluid into advancing hydraulic fractures and reactivated conductive natural cracks or fissures around the wellbore.

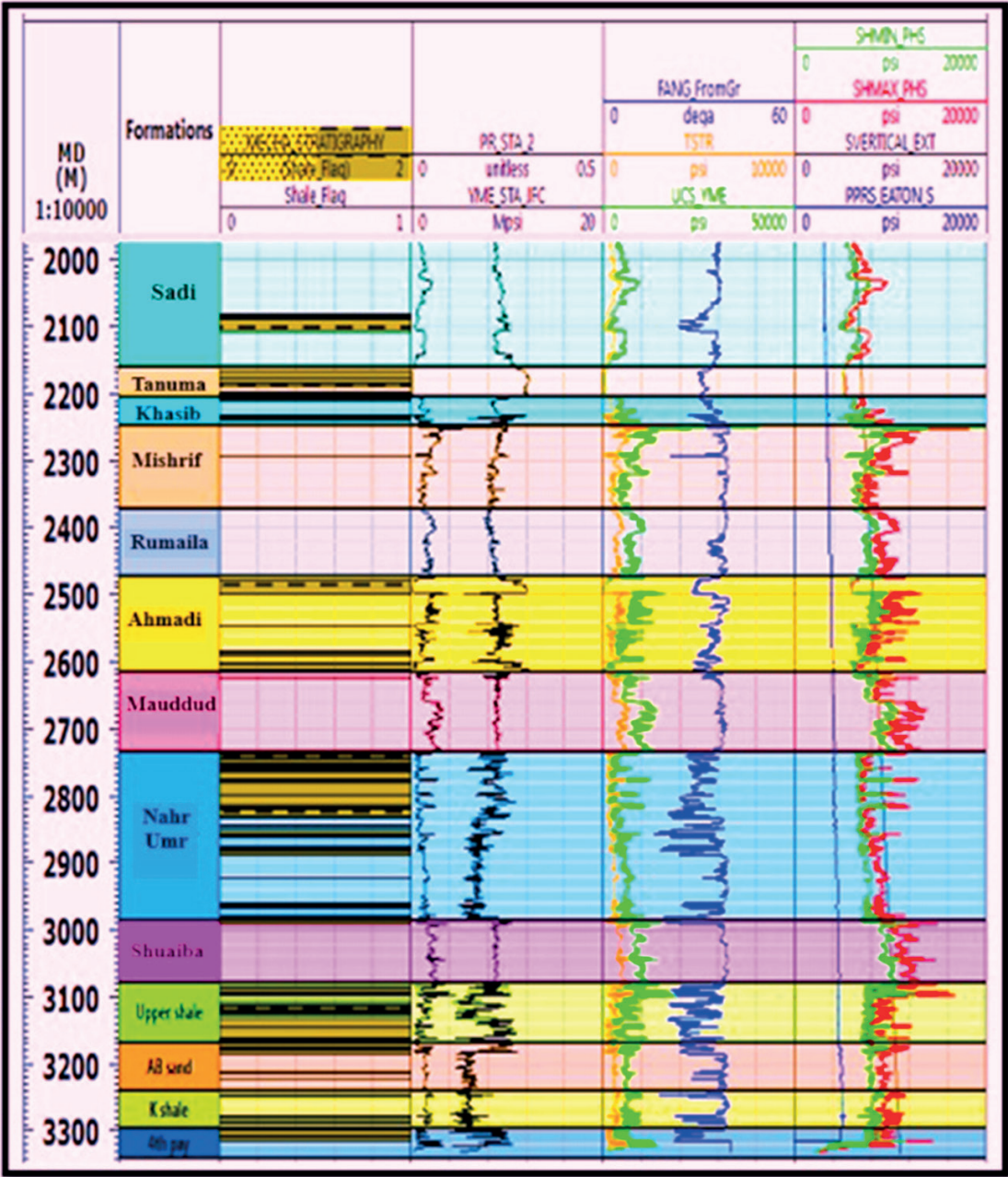


Figure 6. 1D-Geomechanical Model.

Şekil 6. 1D- Jeomekanik Model.

From the above, it can be concluded that the safe mud weight window and a mechanically stable wellbore should be designed so that

the mud weight is above both the shear failure pressure and the pore pressure. Figure 8 shows the relationship between pore pressure, shear



failure pressure, minimum horizontal stress (losses), and formation breakdown pressure with depth. The safe mud weight window is indicated by the shaded green area between the shear failure and the minimum horizontal stress, within which wellbore stability can be maintained while remaining below the formation breakdown pressure and the minimum horizontal stress. Otherwise, the wellbore may become unstable, resulting in significant rock failure and material collapse around the borehole circumference. Then, there is excessive total volume of failed rock material and drilled cuttings and inadequate lifting capacity caused by annulus enlargement. Subsequently, a borehole pack off can occur on the bottom hole assembly. Hence, this condition is sometimes referred to as the lower boundary of the mud weight window, as it indicates that the wellbore has collapsed during drilling, preventing the cuttings from being effectively circulated out of the hole (Figure 9). Wellbore stability analysis starts by determining the rock strength, estimates far-field stress state, and analyzes the stress concentration around the wellbore that is induced due to drilling. All of these parameters are then incorporated into failure criteria in order

to calculate the safe mud weight required to maintain wellbore stability (Noah, et al., 2023).

## RESULTS AND DISCUSSION

### Geomechanical Model Validation

To evaluate the precision of the geomechanical model and to guarantee the outcomes for future well design and field development, each procedure must be validated using actual field data. The validation phase is regarded a crucial stage in the history matching procedure and must be executed prior to model application. Several approaches may be used to diagnose borehole failure, including caliper logging, formation micro-imaging logging (FMI), and analysis of cuttings. Figures 8 to 10 depict wellbore failure anticipated by the failure criteria, namely Modified Lade, Mogi-Coulomb, and Mohr-Coulomb. These metrics delineate the pore pressure, geological attributes, anticipated mud weight range, rock failure, and the true well profile. In each figure below, track 4 delineates the mud weight window, including pore pressure, breakdown, losses, and shear failure, represented in various colors in Table 1 below:

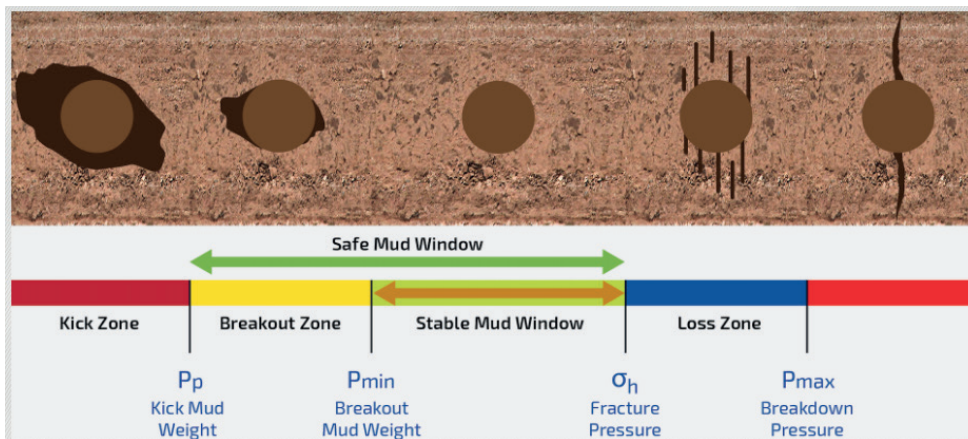


Figure 7. The notion of safe mud weight parameters for drilling (Noah et al., 2023).

Şekil 7. Sondaj için güvenli çamur ağırlığı parametreleri kavramı (Noah ve diğerleri, 2023).



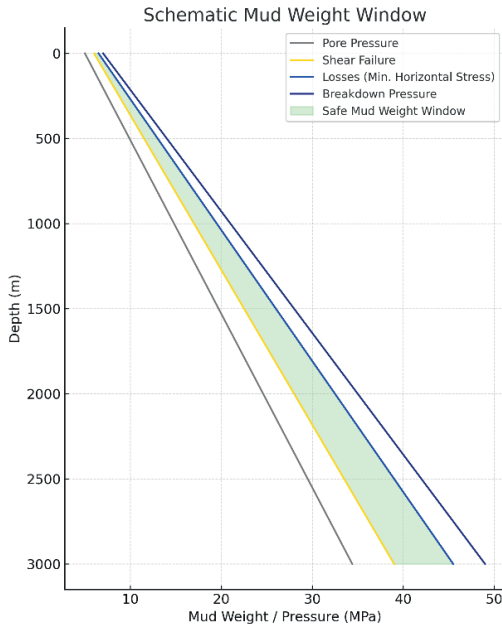


Figure 8. Schematic representation of the mud weight window showing the relationship between pore pressure, shear failure pressure, minimum horizontal stress (losses), and formation breakdown pressure with depth.

Şekil 8. Gözenek basıncı, kesme kırılma basıncı, minimum yatay gerilme (kayıplar) ve formasyon bozulma basıncı ile derinlik arasındaki ilişkiyi gösteren çamur ağırlık penceresinin şematik gösterimi.

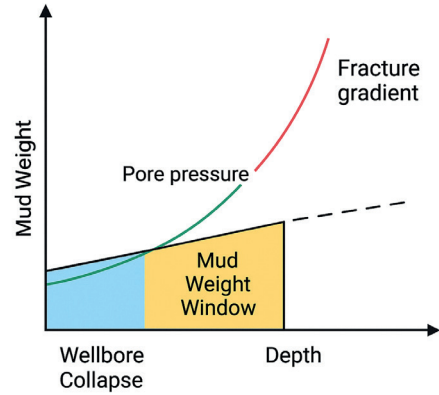


Figure 9. Schematic representation of the mud weight window, illustrating the relationship between pore pressure, fracture gradient, and wellbore collapse as a function of depth (Aadnoy and Looyeh, 2011).

Şekil 9. Gözenek basıncı, kırık gradyanı ve kuyu çökme sınırları arasındaki ilişkiyi derinliğe bağlı olarak gösteren çamur ağırlığı penceresinin şematik gösterimi (Aadnoy ve Looyeh, 2011).

Table 1. The limits of mud weight window.

Çizelge 1. Çamur Ağırlık Penceresinin sınırları.

Property Name	Color code	Description
Pore pressure		Defines the limit of the minimum mud weight required to maintain hydraulic safety.
Shear failure		Defines the minimum mud weight allowed for mechanical stability of the borehole. Below this mud weight, the rock starts to fail, thus intensive breakout occurs.
Losses		When the mud weight pressure (mud density) equals the minimum horizontal stress that causes loss of mud to the fracture formations.
Breakdown		Defines the maximum mud weight allowed for borehole mechanical stability.

To prevent the occurrence of a kick or rock failure on the left side of track 4 in Figures 10-12, the actual mud weight must exceed both the pore pressure (guideline for kick prevention) and the shear failure threshold, indicating the mud weight limit related to shear failure. On the right side of the middle track of the figure, the light blue trend indicates the threshold of mud weight, which indicates the lowest horizontal tension, while the dark blue trend delineates the limit of mud losses and signifies the onset of mud penetration into the formation. To prevent mud losses and breakdown failures, the actual mud weight must be less than the breakdown and loss thresholds. Therefore, to ensure secure operation of drilling procedures and a stable wellbore, the optimal mud weight should be maintained within the intermediate range between the breakout and fracture gradient limits, referred to as the safe mud weight window (SMWW).

Track number 5 in Figures 10-12 outlines the anticipated profile for the rock lowest boundary of mud weight window according to the failure criteria used in this work. The predicted failure differs between red-hued broad breakouts and green-hued shallow knockouts. The well's actual profile was documented and shown by the caliper log and size of the bit, as seen in track 6. Analysis of the projected wellbore instability against the actual rock failure profile reveals a lack of concordance between the two when using the Mohr-Coulomb criterion, likely due to the neglect of intermediate stress factors. The Modified-Lade criterion demonstrates effective matching; nevertheless, it is more cautious about shear failure. The Mogi-Coulomb criterion exhibits closer alignment with the actual wellbore profile obtained from the caliper log at Rumaila oilfield.

### **Interpretation of the mud weight window at specific depths (2800 m and 3000 m):**

To enhance the understanding of how different failure criteria influence the calculated mud weight window (MWW), we analyzed the results at two key depths: 2800 m and 3000 m within the Zubair Formation.

#### **Mud Weight Window at 2800 m Depth:**

*Mohr-Coulomb Criterion:* The calculated mud weight window is relatively narrow. The breakout pressure (shear failure limit) is ~9.8 ppg, while the breakdown pressure (highest boundary of mud weight window) reaches ~13.2 ppg. This suggests a safe drilling range of approximately 3.4 ppg. However, the Mohr-Coulomb criterion tends to underestimate rock strength because it neglects the intermediate principal stress, leading to a conservative (overprotective) estimate of minimum mud weight.

*Mogi-Coulomb Criterion:* At the same depth, the breakout pressure increases to ~10.5 ppg, and the breakdown pressure is around 13.5 ppg, producing a wider and more realistic mud weight window. The inclusion of intermediate stress enhances prediction accuracy, and the result shows better alignment with the observed caliper log breakouts.

*Modified Lade Criterion:* This model gives a breakout pressure of about 10.1 ppg and breakdown pressure around 13.8 ppg, resulting in a broader but more conservative safe margin. The Lade model tends to overestimate the effect of stress triaxiality, resulting in a safer, but perhaps less efficient, drilling window.

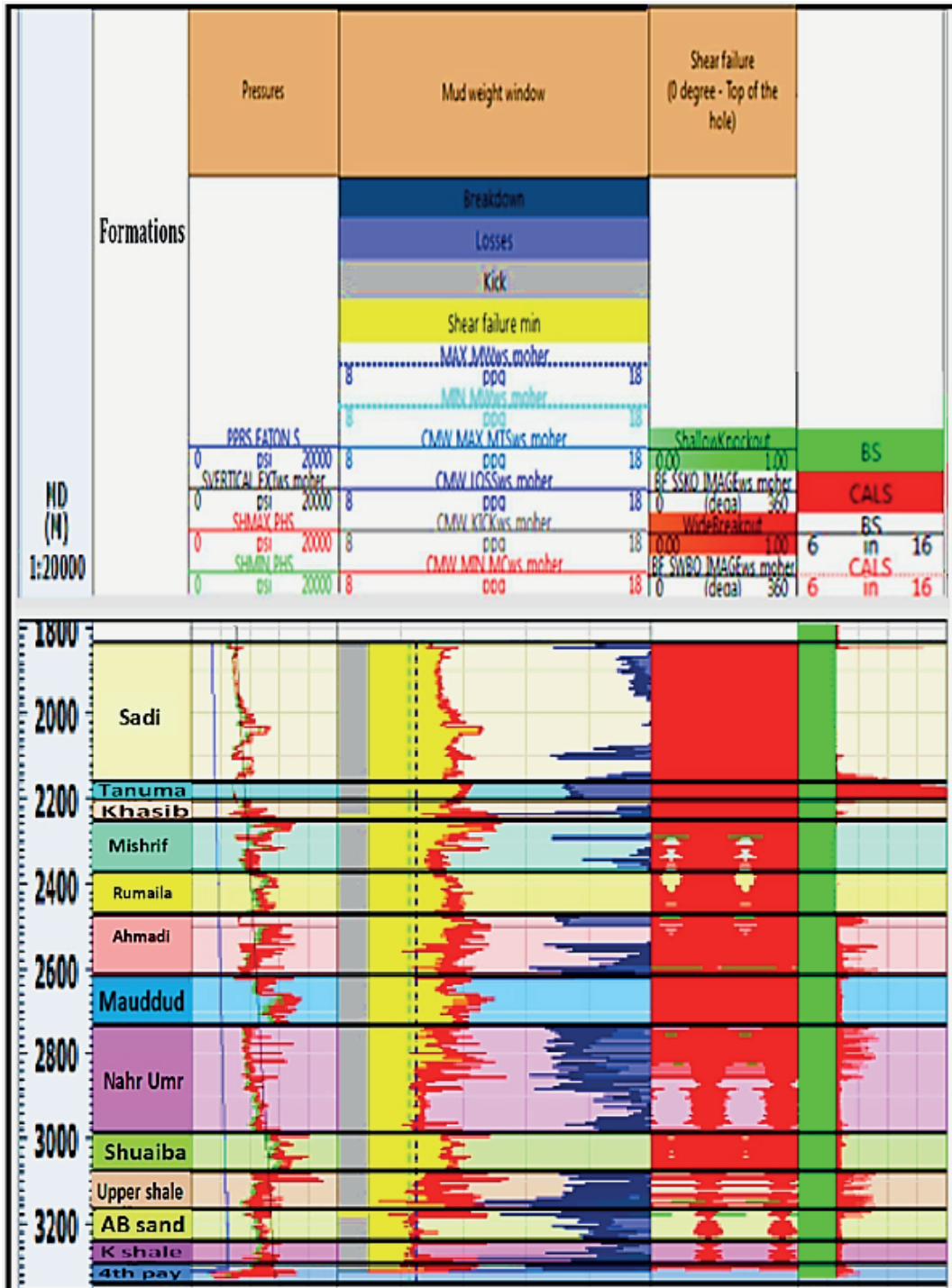


Figure 10. Wellbore failure anticipated by the Mohr-Coulomb failure criterion.

Şekil 10. Mohr-Coulomb yenilme kriteri tarafından öngörülen kuyu çökmesi.

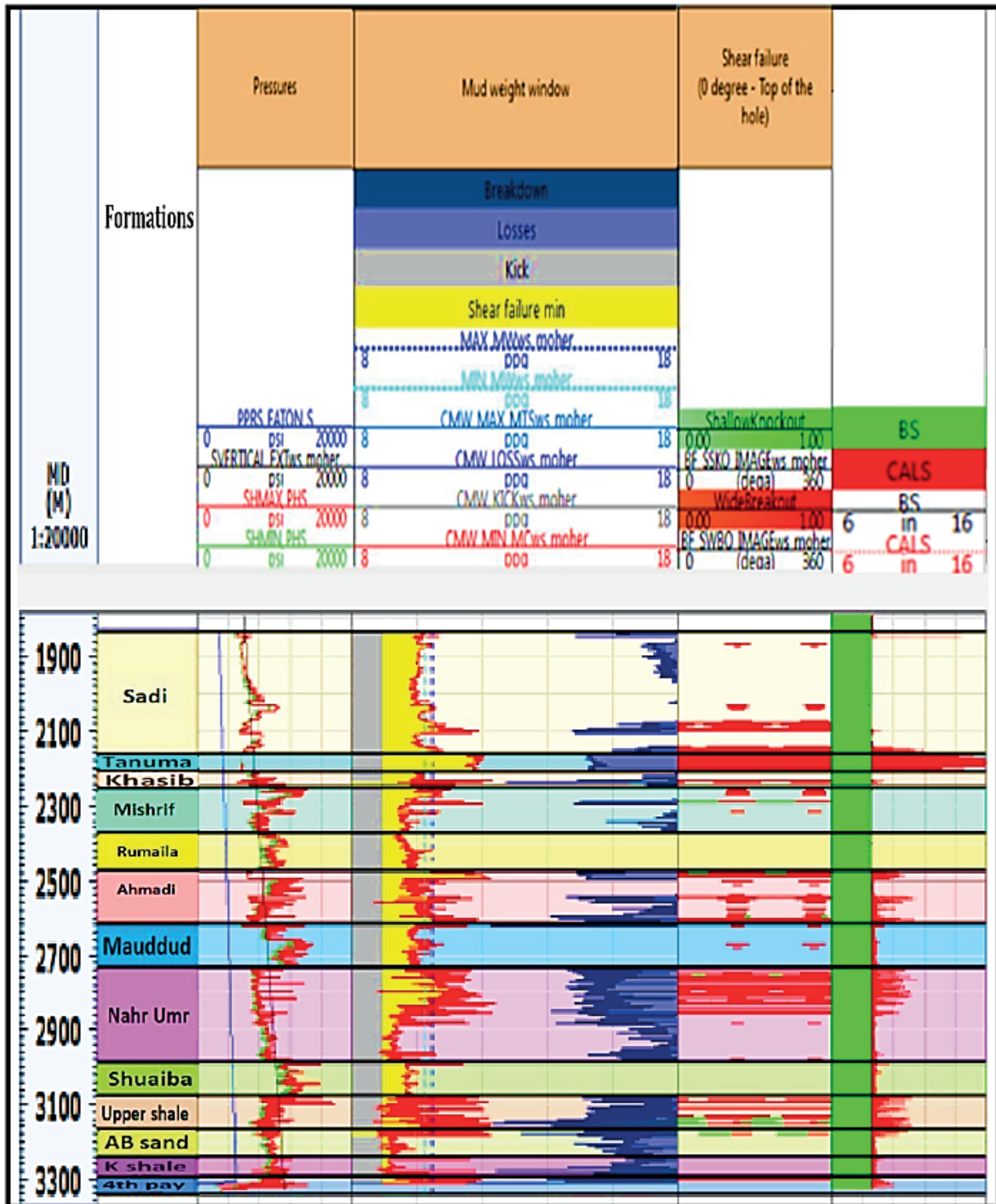


Figure 11. Wellbore failure anticipated by the Mogi-Coulomb failure criterion.

Şekil 11. Mogi-Coulomb yenilme kriteri tarafından öngörülen kuyu çökmesi.



Saadi, Aljuboori, Qader, Shakir, Al-Naemi, Saleh

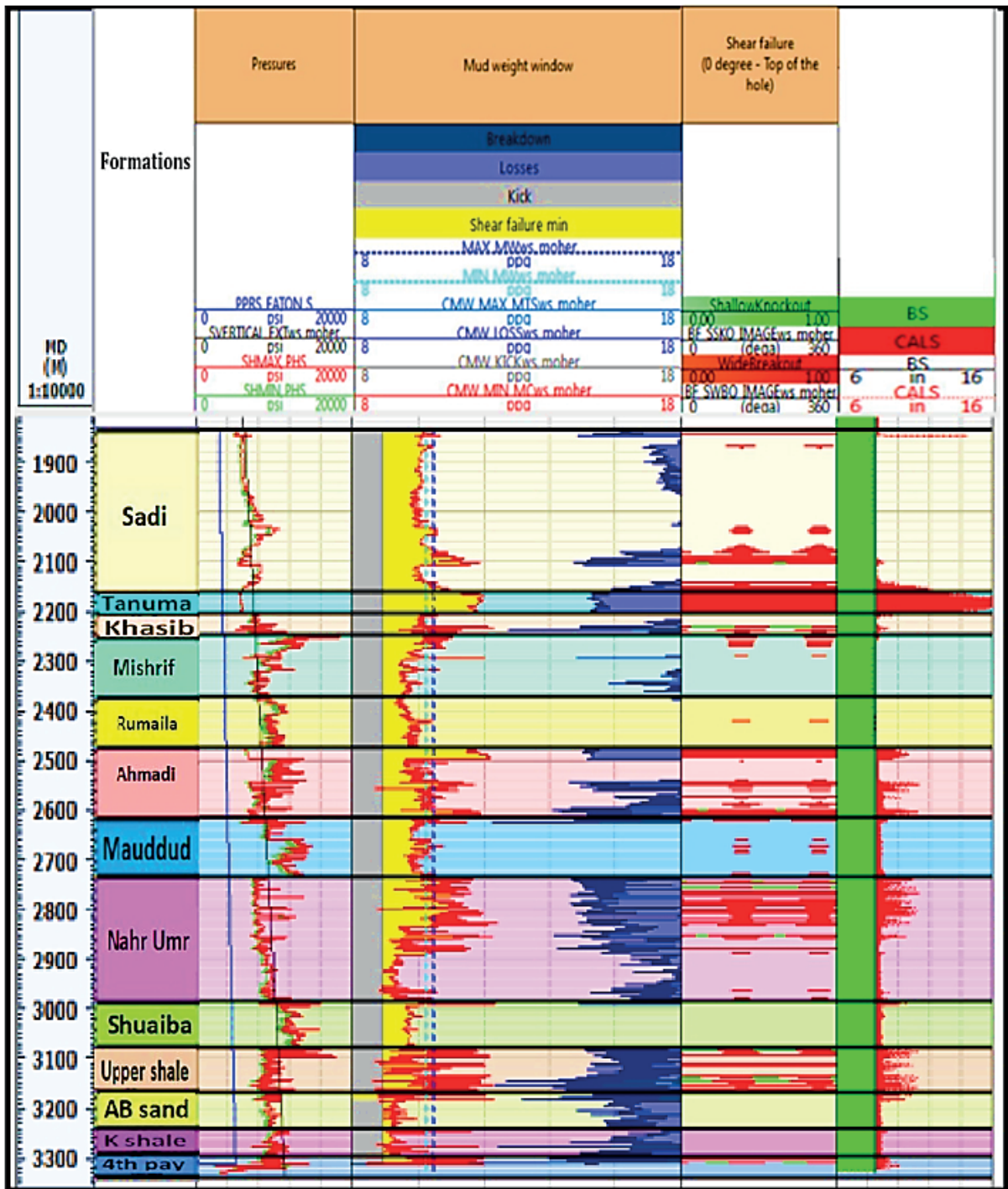


Figure 12. Wellbore failure anticipated by the Modified-Lade failure criterion.

Şekil 12. Değiştirilmiş-Lade yenilme kriteri tarafından öngörülen kuyu çökmesi.



### Mud Weight Window at 3000 m Depth

*Mohr-Coulomb Criterion:* The breakout pressure increases to approximately 10.0 ppg, and breakdown pressure remains close to 13.5 ppg, keeping the safe window around 3.5 ppg. The narrow window reflects its limitation in representing real subsurface conditions at this deeper depth. *Mogi-Coulomb Criterion:* A breakout pressure of 10.7 ppg and breakdown pressure of 13.7 ppg is observed. This criterion continues to reflect a more balanced and accurate representation of wellbore stability, making it a suitable choice for high-stress environments like Rumaila.

*Modified Lade Criterion:* At this depth, the breakout pressure is close to 10.3 ppg with the breakdown limit extending to 14.0 ppg, again demonstrating a more conservative profile similar to its behavior at 2800 m.

### Impact of Failure Criterion on Mud Weight Window

*Mohr-Coulomb criterion:* While simple and widely used, this criterion yields conservative and potentially inefficient drilling windows, especially in deep and high-stress zones. *Mogi-Coulomb Criterion:* This proves to be most representative of actual borehole behavior, as confirmed by caliper logs. It balances safety and operational efficiency and accounts for the intermediate principal stress, which becomes more influential at greater depths.

*Modified Lade criterion:* This is more conservative, typically providing wider upper safety margins. This makes it appropriate for brittle or fractured formations where failure prediction is critical but may result in overdesign in more competent formations.

### Sensitivity Analysis and Mud Weight Window

The borehole data necessary for performing analysis of sensitivity at a certain depth include well orientation, geomechanical model parameters, and the mud weight. Due to increased brittleness and susceptibility to fracturing of sandstone, induced-tensile failure and mud losses are likely to occur. Shale is more likely to develop breakout compared with sandstone. The sensitivity analysis of mud weight window showed that the safe mud weight is below 40° and mud weight range is 10.5 to 14.2 ppg. The azimuth had zero effect on the mud weight as shown in Figures 13 and 14.

### CONCLUSIONS

The following findings can be drawn from the outcomes of the 1D MEM analysis for the Zubair Formation/Rumaila oilfield:

1. To achieve an accurate 1D-MEM, integrated data is required such as well logs (caliper log, bit size, sonic log, gamma ray and bulk density) and drilling formation data (daily drilling report, final drilling report, geological report). Measured data are essential for validation of the constructed model.
2. The Mohr-Coulomb criterion appeared overstate rock failure, while the Modified-Lade criterion was conservative in predicting rock failure. The Mogi-Coulomb criterion was more reasonable and appropriate in predicting rock failure for Rumaila oilfield and showed good agreement with the breakouts observed in logs because it considers intermediate principal stress when analyzing failure.

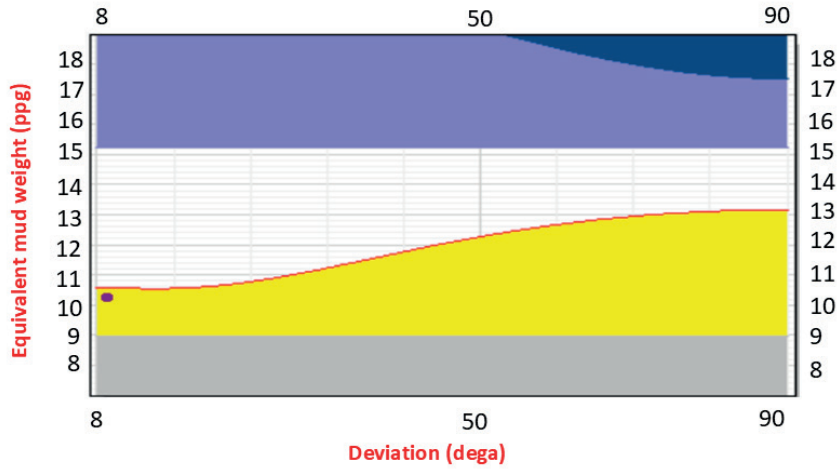


Figure 13. Mud weight window vs. deviation.

Şekil 13. Çamur ağırlık penceresi ve sapma.

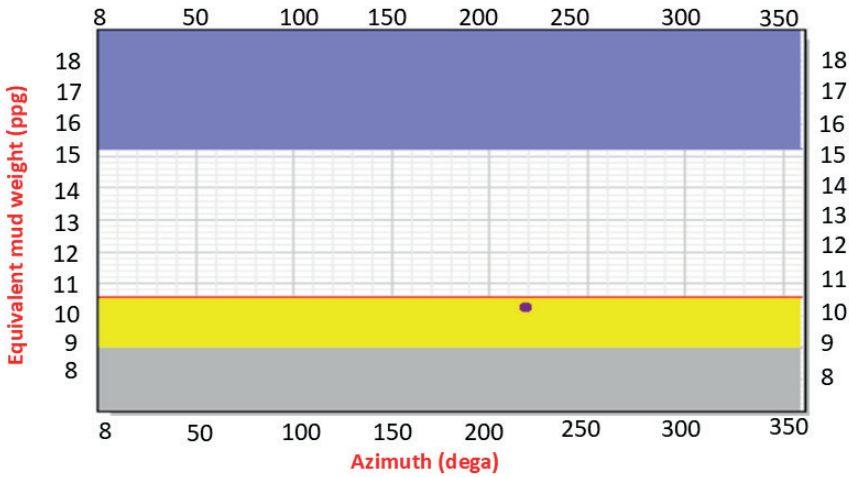


Figure 14. Mud weight window vs. azimuth.

Şekil 14. Çamur ağırlığı penceresi ve Azimut.

3. Sensitivity analysis indicated that vertical and minimally deviated wells exhibit greater stability than horizontal and deviated wells. Furthermore, the current mud weight is inadequate and must be elevated to 10.5 ppg in order to ensure the stability of the wellbore wall during drilling operations.

These findings may be used to mitigate the elevated NPT and excessive costs associated with well drilling operations.

4. Vertical and low-deviation wells with less than 40° exhibit greater stability than highly deviated and horizontal wells (from Sadi to Zubair Formation), which is based on

the results of sensitivity analysis at a single depth.

5. Ultimately, the appropriate and best failure criterion should be chosen for use in building a geomechanical model to create drilling programs. This step is crucial for planned wells and making real-time revisions to those programs has proven valuable when successfully drilling hazardous intervals, simultaneously reducing costs and duration of the planned well delivery.

## RECOMMENDATIONS

For future work, the recommendations can be listed as following:

1. Based on these study components, a strong three-dimensional geomechanical model (3D MEM) should be developed that will greatly integrate the mechanical earth model and the structural geology model to give a more thorough and accurate evaluation of wellbore stability.
2. It is recommended to study the chemical effects of the mud.
3. The values for minimal horizontal stresses should be corrected by performing further leak-off tests or extended leak-off tests at various intervals.

## REFERENCES

- Aadnoy, B. and Looyeh, R., (2011). *Petroleum rock mechanics: drilling operations and well design*. Gulf Professional Publishing.
- Aadnoy, B. and Looyeh, R., (2019). *Petroleum Rock Mechanics Drilling Operations and Well Design* Second Edition. Gulf Professional Publishing.
- Abalioglu, I., Legarre, H., Garland, C., Sallier, B., Gao, J., van Galen, M., Chou, Q., Neil, B., Soroush, H., Qutob, H., Mahli, Z., (2011). *The role of geomechanics in diagnosing drilling hazards and providing solutions to the northern Iraq fields*, in: SPE Middle East Oil and Gas Show and Conference, SPE, pp. SPE-142022, <https://doi.org/10.2118/142022-MS>.
- Al-Agaili, H. E. C. (2012). *Palynofacies and hydrocarbon potential for selected samples from Subba oil field, south Iraq*. University of Baghdad, Baghdad.
- Al-Ajmi, A. M., and Zimmerman, R. W. (2006). Stability analysis of vertical boreholes using the Mogi–Coulomb failure criterion, *International Journal of Rock Mechanics and Mining Sciences*, vol 43, pp .1200-1211, <https://doi.org/10.1016/j.ijrmms.2006.04.001>.
- Al-Ameri N. J., Hamd-allah S, Abass H. (2020b). *Investigating geomechanical considerations on suitable layer selection for hydraulically fractured horizontal wells placement in tight reservoirs*. In: Abu Dhabi international petroleum exhibition and conference (ADIPEC). SPE-203249-MS, <https://doi.org/10.2118/203249-MS>.
- Al-Ameri N. J., Hamd-allah S, Abass H. (2020c). Specifying quality of a tight oil reservoir through 3-D reservoir modeling. *Iraqi Journal of Science*, 61(12), 3252–3265, <https://doi.org/10.24996/ij.s.2020.61.12.14>.
- Al-Ameri, N. J. (2015). Kick tolerance control during well drilling in southern Iraqi deep wells. *IJCPE*, vol. 16, no. 3, pp. 45–52, <https://doi.org/10.31699/IJCPE.2015.3.5>.
- Algburi, A., Alatrosh, R. K., and Alrashedi, M. A., (2023). Study of Hydrocarbon Potentials and Sedimentary Properties of Ispartaçay Formation, Turkey. *Iraqi Geological Journal*. Vol. 56 (2C), 33-49. DOI: <https://doi.org/10.46717/igj.56.2C.3ms-2023-9-9>.
- AlHusseini, A. K. & Hamed-Allah, S. M. (2023). Estimation Pore and Fracture Pressure Based on Log Data; Case Study: Mishrif Formation/ Buzurgan Oilfield at Iraq. *IJCPE*, vol. 24, no. 1, pp. 65–78, <https://doi.org/10.31699/IJCPE.2023.1.8>.
- Ali, R., A. (2023). Petrography and Geochemistry of Zubair Shale Formation in Rumaila oilfield

Saadi, Aljuboori, Qader, Shakir, Al-Naemi, Saleh

- southern Iraq: implications for provenance and tectonic setting. *JPRS*, Volume No. 40, pp. 19-40. <http://doi.org/10.52716/jprs.v13i3.729>.
- Al-Juraisy, B.A. and Al-Majid, M.H.A. (2021). Importance of Velocity Deviation Technique and Negative Secondary Porosity in Detection of Hydrocarbon Zones in Khasib Formation, East Baghdad Oil Field. *Iraqi Geological Journal*. Vol. 54 (2E), 86-103. DOI: <https://doi.org/10.46717/igj.54.2E.6Ms-2021-11-22>.
- Almasi, A., and Mohsenipour, A. (2022). Determining the mud window, geomechanical model (MEM), and well wall stability analysis, using analytical and numerical methods in one of the wells in Iran's southwest fields, *Advanced Applied Geology* 12 (1), 1–11. DOI:10.22055/AAG.2020.34229.2135.
- Al-Qahtani, M. Y., and Zillur, R. (2001). *A mathematical algorithm for modeling geomechanical rock properties of the Khuff and Pre-Khuff reservoirs in Ghawar field*, in: SPE Middle East Oil and Gas Show and Conference, pp. SPE–68194. SPE.
- Al-Rubaye W. I. T., and Hamd-Allah, S. M. (2019). A High Resolution 3D Geomodel for Giant Carbonate Reservoir- A Field Case Study from an Iraqi Oil Field. *Jcoeng*, vol. 26, no. 1, pp. 160–173, 2019, <https://doi.org/10.31026/j.eng.2020.01.12>.
- AlShibli, F. H., and Alrazzaq, A. A. A. (2022). Laboratory Testing and Evaluating of Shale Interaction with Mud for Tanuma Shale formation in Southern Iraq. *IJCPE*, vol. 23, no. 3, pp. 35–41, <https://doi.org/10.31699/IJCPE.2022.3.5>.
- Bagheri, H., Ayatizadeh Tanha, A., Doulati Ardejani, F., Heydari-Tajareh, M., and Larki, E. (2021). *Geomechanical model and wellbore stability analysis utilizing acoustic impedance and reflection coefficient in a carbonate reservoir*, *J. Pet. Explor. Prod. Technol.* 11, 3935–3961.
- Balaky S. M., Al-Dabagh M. M., Asaad I. S., Tamar-Agha M., Ali M. S., Radwan A. E. (2023). Sedimentological and petrophysical heterogeneities controls on reservoir characterization of the Upper Triassic shallow marine carbonate Kurra Chine Formation, Northern Iraq: Integration of outcrop and subsurface data. *Mar Pet Geol.* 149. doi:10.1016/j.marpetgeo.2022.106085.
- Bandara, M. K. and Al-Ameri, N. J. (2024). Wellbore Instability Analysis to Determine the Safe Mud Weight Window for Deep Well, Halfaya Oilfield. *Iraqi Geological Journal*. vol. 57 (1D), 153-173. DOI:10.46717/igj.57.1D.13ms-2024-4-23.
- Bell, J. S. (2003). Practical methods for estimating in situ stresses for borehole stability applications in sedimentary basins. *Journal of Petroleum Science and Engineering* vol. 38, pp. 111–119, [https://doi.org/10.1016/S0920-4105\(03\)00025-1](https://doi.org/10.1016/S0920-4105(03)00025-1).
- Boutt, D. F., Cook, B. K. and Williams, J. R. (2011). A coupled fluid–solid model for problems in geomechanics: Application to sand production, *International Journal for Numerical and Analytical Methods in Geomechanics*, vol.35, pp. 997-1018, <https://doi.org/10.1002/nag>.
- Bradley, W. B. (1979). Failure of inclined boreholes, *J. Energy Resour. Technol. Trans. ASME*, vol. 101, no. 4, pp. 232–239, 1979, <https://doi.org/10.1115/1.3446925>.
- Chandong, C., Zoback, M. D. and Khaksar, A. (2006). Empirical Relations between Rock Strength and Physical Properties in Sedimentary Rocks. *Journal of Petroleum Science and Engineering*, vol.51, pp.223–237, <https://doi.org/10.1016/j.petrol.2006.01.003>.
- Ding, Y., Liu, X., Liang, L., Xiong, J., Li, W., Wei, X., Duan, X., and Hou, L. (2023). Wellbore stability model in shale formation under the synergistic effect of stress unloading-hydration. *Pet. Explor. Dev.* 50 (6), 1478-1486.
- Ewy, R.T. (1999). Wellbore-Stability Predictions by Use of a Modified Lade Criterion,” *SPE Drill & Compl*, vol. 14, pp. 85–91, <https://doi.org/10.2118/56862-Pa>.
- Fischer, K., Henk, A. (2013). A workflow for building and calibrating 3-D geomechanical models &ndash a case study for a gas reservoir in the North German Basin, *Solid Earth* 4 347–355.
- Gstalter, S. and Raynal, J. (1966). Measurement of Some Mechanical Properties of Rocks And

- Their Relationship to Rock Drillability, *J. Pet. Technol.*, vol. 18, no. 08, pp. 991–996, <https://doi.org/10.2118/1463-Pa>.
- Herwanger, J. (2014). *Seismic geomechanics: how to build and calibrate geomechanical models using 3D and 4D seismic data*, in: Fourth EAGE CO2 Geological Storage Workshop, European Association of Geoscientists & Engineers, 2014 cp-439.
- Hoseinpour M. and Riahi, M. A. (2022). Determination of the mud weight window, optimum drilling trajectory, and wellbore stability using geomechanical parameters in one of the Iranian hydrocarbon reservoirs. *J Petrol Explor Prod Technol*, vol.12, pp. 63–82, <https://doi.org/10.1007/s13202-021-01399-5>.
- Hosseini, S. A., Keshavarz Faraj Khah, N., Kianoush, P., Arjmand, Y., Ebrahimabadi, A., Jamshidi, E. (2023b). Tilt angle filter effect on noise cancellation and structural edges detection in hydrocarbon sources in a gravitational potential field. *Results Geophys. Sci.* 14, 100061, <https://doi.org/10.1016/j.ringps.2023.100061>.
- Kianoush, P., Mohammadi, G., Hosseini, S. A., Keshavarz Faraj Khah, N., Afzal, P. (2023b). Determining the drilling mud window by integration of geostatistics, intelligent, and conditional programming models in an oilfield of SW Iran. *J. Pet. Explor. Prod*, <https://doi.org/10.1007/s13202-023-01613-6>.
- Liu J, Ma T, Fu J, Gao J, Martyushev D. A., Ranjith PG. (2024). Thermodynamics based unsaturated hydro-mechanical-chemical coupling model for wellbore stability analysis in chemically active gas formations. *Journal of Rock Mechanics and Geotechnical Engineering*, <https://doi.org/10.1016/j.jrmge.2024.09.024>.
- Ma, T., Chen, P. (2015). A wellbore stability analysis model with chemical-mechanical coupling for shale gas reservoirs. *J. Nat. Gas Sci. Eng.* 26, 72–98, <https://doi.org/10.1016/j.jngse.2015.05.028>.
- Ma, T., Chen, P., Yang, C., and Zhao, J. (2015). Wellbore stability analysis and well path optimization based on the breakout width model and Mogi-Coulomb criterion. *J. Pet. Sci. Eng.* 135, 678–701, <https://doi.org/10.1016/j.petrol.2015.10.029>.
- Manshad, A. K., Ali, J., Aghayari, M., Hayavi, M. T., Mohammadi, A. H., Iglauer, S., and Keshavarz, A. (2022). *An insight into modeling wellbore stability using the extended Mogi-Coulomb criterion and poly-axial test data*. Upstream Oil Gas Technol. Vol. 9, 100082, <https://doi.org/10.1016/j.upstre.2022.100082>.
- Mohiuddin, M. A., Awal, M. R., Abdulraheem, A., and Khan, K. (2001). *A new diagnostic approach to identify the causes of borehole instability problems in an offshore Arabian field*, in: SPE Middle East Oil and Gas Show and Conference, SPE, pp. SPE–68095, <https://doi.org/10.2118/68095-MS>.
- Moos, D., Peska, P., Finkbeiner, T., and Zoback, M. (2003). Comprehensive wellbore stability analysis utilizing Quantitative Risk Assessment. *J. Pet. Sci. Eng.*, vol. 38, pp. 97–109, [https://doi.org/10.1016/S0920-4105\(03\)00024-X](https://doi.org/10.1016/S0920-4105(03)00024-X).
- Nader, A. F., Muhammad, R., J., Saleh, W., M., Abdullah, M., S., and Atwan, A., Q. (2022). evaluation of main Pay-Zubair Formation after operations re-injection of produced water directly in Rumaila oil field norths under matrix condition. *Journal of Petroleum Research and Studies*. Volume No. 35, pp. 13-26. <http://doi.org/10.52716/jprs.v12i2.655>.
- Noah, A. Z., Mesbah, M. A., and Osman, H. (2023). Comprehensive Wellbore Instability Management by Determination of Safe Mud Weight Windows Using Mechanical Earth Model, Meleiha Field, Western Desert, Egypt. *Egyptian Journal of Chemistry*, vol. 66, pp. 449–463, [doi.org/10.21608/ejchem.2022.150856.6534](https://doi.org/10.21608/ejchem.2022.150856.6534).
- Ounegh, A., Hasan-Zadeh, A., Khanaposhtani, M. M., and Kazaemzadeh, Y. (2024). Wellbore stability analysis based on the combination of geomechanical and petrophysical studies. *Results in Engineering*. Vol. 24, 103016, <https://doi.org/10.1016/j.rineng.2024.103016>.
- Pirhadi, A., Kianoush, P., Ebrahimabadi, A., and Shirinabadi, R. (2023). Wellbore stability in a depleted reservoir by finite element analysis of coupled thermo-poro-elastic units in an oilfield, SW Iran. *Results in Earth Sciences journal*. Vol. 1, 100005, <https://doi.org/10.1016/j.rines.2023.100005>.



- Plumb, R.A., and Richard, S. H. (1985). Stress-induced borehole elongation: A comparison between the four-arm dipmeter and the borehole televiwer in the Auburn Geothermal Well. *Journal of Geophysical Research*, vol. 90, pp. 5513–5521, <https://doi.org/10.1029/JB090iB07p05513>.
- Rafieepour, S., Zamiran, S., and Ostadhassan, M. (2020). A cost-effective chemo-thermo-poroelastic wellbore stability model for mud weight design during drilling through shale formations. *J. Rock Mech. Geotech. Eng.* 12 (4), 768-779, <https://doi.org/10.1016/j.jrmge.2019.12.008>.
- Ramjohn, R., Gan, T., Sarfare, M. (2018). *3D geomechanical modeling for wellbore stability analysis: starfish*, ECMA, Trinidad and Tobago, in: SPE Trinidad and Tobago Section Energy Resources Conference, SPE, D031S027R002, <https://doi.org/10.2118/191242-MS>.
- Rumaila Operating Organization, ROO. (2016). *Integrated Subsurface Description* (unpublished report).
- Schlumberger, 2018. *Techlog Software Manual*.
- Wang, Y., Duan, L., Zhang, F., Lian, M., and Li, B. (2023). Dynamic wellbore stability analysis based on thermo-poro-elastic model and quantitative risk assessment method. *Geoenergy Sci. Eng.*, 212063, <https://doi.org/10.1016/j.geoen.2023.212063>.
- Wei, Y., Feng, Y., Tan, Z., Yang, T., Yan, S., Li, X., and Deng, J. (2024). Simultaneously improving ROP and maintaining wellbore stability in shale gas well: A case study of Luzhou shale gas reservoirs. *Rock Mech. Bull.* 3 (3), 100124, <https://doi.org/10.1016/j.rockmb.2024.100124>.
- Yan, C., Dong, L., Zhao, K., Cheng, Y., Li, X., Deng, J., Li, Z., and Chen, Y. (2022). Time-dependent borehole stability in hard-brittle shale. *Pet. Sci.* 19 (2), 663-677, <https://doi.org/10.1016/j.petsci.2021.12.019>.
- Zeynali, M. E. (2012). Mechanical and physico-chemical aspects of wellbore stability during drilling operations. *J. Pet. Sci. Eng.* 82, 120-124, <https://doi.org/10.1016/j.petrol.2012.01.006>.
- Zhang, J. (2013). Borehole stability analysis accounting for anisotropies in drilling to weak bedding planes. *International Journal of Rock Mechanics and Mining Sciences* 60, 160–70, <https://doi.org/10.1016/j.ijrmms.2012.12.025>.
- Zoback, M. D., Moos, D., Mastin, L., and Anderson, R. N. (1985). Well bore breakouts and in situ stress, *J. Geophys. Res. Solid Earth* 90, 5523–5530, <https://doi.org/10.1029/JB090iB07p05523>.